Available online at www.sciencedirect.com

SciVerse ScienceDirect

Magnetic Resonance Imaging 30 (2012) 1167–1176

MAGNETIC RESONANCE IMAGING

Metabolic profile of dystrophic *mdx* mouse muscles analyzed with in vitro magnetic resonance spectroscopy (MRS)

Aurea B. Martins-Bach[a], Antonio C. Bloise[a], Mariz Vainzof[b], Said Rahnamaye Rabbani[a,*]

[a]*Magnetic Resonance Laboratory, Physics Institute, University of São Paulo, CEP 05508-090, São Paulo, Brazil*

[b]*Muscle Protein and Comparative Histopathology Laboratory, Human Genome Research Center, Department of Biology, Biosciences Institute, University of São Paulo, CEP 05508-090, São Paulo, Brazil*

Received 24 August 2011; revised 13 March 2012; accepted 2 April 2012

Abstract

Duchenne muscular dystrophy (DMD) is a recessive X-linked form of muscular dystrophy characterized by progressive and irreversible degeneration of the muscles. The *mdx* mouse is the classical animal model for DMD, showing similar molecular and protein defects. The *mdx* mouse, however, does not show significant muscle weakness, and the diaphragm muscle is significantly more degenerated than skeletal muscles. In this work, ^{1}H magnetic resonance spectroscopy (MRS) was used to study the metabolic profile of quadriceps and diaphragm muscles from *mdx* and control mice. Using principal components analysis (PCA), the animals were separated into groups according to age and lineages. The classification was compared to histopathological analysis. Among the 24 metabolites identified from the nuclear MR spectra, only 19 were used by the PCA program for classification purposes. These can be important key biomarkers associated with the progression of degeneration in *mdx* muscles and with natural aging in control mice. Glutamate, glutamine, succinate, isoleucine, acetate, alanine and glycerol were increased in *mdx* samples as compared to control mice, in contrast to carnosine, taurine, glycine, methionine and creatine that were decreased. These results suggest that MRS associated with pattern recognition analysis can be a reliable tool to assess the degree of pathological and metabolic alterations in the dystrophic tissue, thereby affording the possibility of evaluation of beneficial effects of putative therapies.

Keywords: Duchenne muscular dystrophy; *mdx*; High-resolution ^{1}H MRS; Metabolomics

1. Introduction

Duchenne muscular dystrophy (DMD) is the most common and severe X-linked progressive muscular dystrophy in men [1], affecting 1:3500 living male newborns. The symptoms of weakness start at around the age of 3 years, with frequent falls and difficulties to climb stairs, and the progression of the disease results in loss of ambulation at about the age of 10 years. Patients usually die at around 20–30 years of age due to heart or respiratory failure [1–3]. Approximately 30% of patients present with a variable degree of mental retardation [4].

DMD is caused by deletions, duplications or non-sense mutations in the dystrophin gene which result in the absence of dystrophin in the muscle fiber membrane [5]. Dystrophin is a subsarcolemmal protein present in skeletal and cardiac muscle cells and also in some nervous cells, such as cortical and hippocampal neurons and Purkinje cells [6]. This protein is part of the dystrophin–glycoprotein complex (DGC), an oligomeric complex of proteins and glycoproteins. DGC plays an important structural role in muscle fibers, connecting the subsarcolemmal cytoskeleton, through actin filaments, to the extracellular matrix [7–9]. Absence of DGC's components causes different types of dystrophies, and particularly, the absence of dystrophin causes muscle fiber's gradual degeneration and replacement by adipose and conjunctive tissue, which lead to progressive loss of muscular strength [2,3]. Typical histopathological findings in the DMD patient's muscle are rounding of the fibers, diffuse variation in fiber size, necrosis and subsequent loss of

* Corresponding author. Instituto de Física da Universidade de São Paulo (IFUSP), Rua do Matão, Travessa R, 187, CEP 05508-090, São Paulo/SP, Brazil. Tel.: +55 11 3091 6689; fax: +55 11 3814 0503.

E-mail address: srabbani@if.usp.br (S. Rahnamaye Rabbani).

0730-725X/$ – see front matter © 2012 Elsevier Inc. All rights reserved.
doi:10.1016/j.mri.2012.04.003

fibers, basophilic regenerating fibers, increased internal nuclei, and infiltration by connective and adipose tissues [10].

The most frequently used animal model for DMD is the *mdx* mouse, which has a point mutation in the dystrophin gene and absence of this protein in the muscle fibers. However, the muscular impairment and the histological findings are milder than those observed in DMD patients [11,12]. The diaphragm muscle of the *mdx* mouse is significantly more degenerated than other skeletal muscles, with degenerative characteristics of the human DMD muscle [13]. There is no cure to DMD; however, different therapeutic strategies are in development, and a noninvasive method to follow their possible clinical benefits would have a great value [14–16].

When applied to the study of DMD, ^{1}H magnetic resonance spectroscopy (MRS) has been shown to be an efficient method to identify metabolic changes in muscle and serum, allowing a better understanding of some biochemical processes induced by the disease [17–23]. In this paper, ^{1}H high-resolution MRS analysis was used to study two muscles with a different pattern of degeneration in the adult *mdx* mouse: the diaphragm and the femoral quadriceps. These muscles were analyzed at two stages of degeneration: at ages of 3 and 6 months for both *mdx* and control mice. This analysis identified alterations in the levels of certain metabolites in the dystrophic process of the *mdx* mouse. Tracking the metabolic profile of muscle degeneration due to dystrophin deficiency was evident even when the histological analysis did not show major differences.

2. Methods and materials

Mice were obtained from the animal house of the Human Genome Research Center, Bioscience Institute of São Paulo University. The colonies received the routine required care for good health, including controlled environment with central air-conditioning and room temperature at 22°C, artificial illumination cycled at 12-h intervals, and food and water ad libitum. Forty-five animals were studied: 12 C57Bl/*mdx* (*mdx*) and 11 C57Bl/wild (*ctrl*) mice at 3 months of age and 12 *mdx* and 10 *ctrl* mice at 6 months of age. Animals were euthanized using CO_2 chamber; the quadriceps and diaphragm muscles were dissected and divided into two parts, one for histology and the other for nuclear MR (NMR) study. Histology samples were cryoprotected and frozen in N_2 liquid, where they remained until use. NMR samples were frozen in N_2 liquid and stored at −70°C until use. The experimental procedures were approved by the Ethics Committee of Animal Experiments (protocol no. 006/53) from the Biomedical Sciences Institute of São Paulo University.

2.1. Histologic analysis

The histology samples were mounted in Tissue-Tek O.C.T. (Optimal Cutting Temperature, Sakura) embedding medium and cut in a cryostat microtome to obtain 5-μm-thick slices in the rostrocaudal direction. The slices were cut at temperatures below −20°C and were mounted in glass slides with poly-L-lysine and stained with hematoxylin and eosin. Histological evaluation was performed with a light microscope to compare the principal characteristics of the dystrophy: degeneration–regeneration focus, necrosis, and infiltration by connective and adipose tissues. The histology analysis was performed to qualitatively compare the groups.

2.2. NMR samples preparation

Quadriceps samples were homogenized in 2 ml of acetonitrile:distilled water solution (1:1) [24] and centrifuged at 6100*g* and 4°C for 40 min, and the supernatants were lyophilized. The obtained powder was resuspended in 0.7 ml of deuterium oxide with trimethylsilyl propionate acid sodium salt (TSP, Sigma) at 10 mM. TSP was used as a chemical shift and concentration internal reference. Due to the smaller collected masses of diaphragm muscle, the tissue was homogenized in 1 ml of acetonitrile:distilled water solution and centrifuged at the same speed and temperature used for quadriceps samples but for a longer time (160 min, 4°C). All the sample preparation procedures were done at temperatures ≤4°C.

2.3. NMR spectroscopy

High-resolution ^{1}H NMR spectra were acquired in a Varian spectrometer (Varian Associated, Inc., Palo Alto, CA, USA) operating at 200 MHz and 21°C. For one-dimensional (1D) spectroscopy, pulse sequence parameters were as follows: relaxation delay 10 s, excitation pulse width 12 μs, acquisition time 14.8 s, spectral window 1.4 kHz, 64k data points and 256 transients. A weighted Fourier transformation with line broadening apodization function of 0.3 Hz was applied to the spectra, followed by phase and baseline correction. Homonuclear correlation spectra (COSY-45) were acquired to unambiguously identify the metabolites related to the observed peaks. The two-dimensional spectroscopy parameters were as follows: relaxation delay 5 s; 90° and 45° pulse width 20 and 10 μs, respectively; acquisition time 1.46 s; spectral window in both dimensions (F1 and F2) 1.4 kHz; 4k data points for F2 dimension; 64 data points for F1 dimension (indirect dimension) and 44 transients. Spectra were Fourier transformed using sine-bell function and 0.3 Hz exponential (F1 and F2) line broadening function.

2.4. Statistics and pattern recognition processing of data

The region from 4.5 to 5.1 ppm of 1D spectra, overlapping the water absorption, was excluded, and the vertical scale was normalized by the TSP area (−0.07 to 0.07 ppm). The spectra were also normalized by its total area excluding the TSP region to eliminate the concentration variability observed in different samples. The observed resonance peaks were identified based on the literature

[17,19,22] and COSY experiments. The peaks were automatically integrated and directly compared between *mdx* and *ctrl* mice using the nonparametric Kruskal–Wallis test. If $P \leq .05$, the Dunn's test for multiple comparison was applied. After the analysis, the significance level was adjusted by the Bonferroni's correction for the 48 tests performed, and differences were considered statistically significant if $P \leq .001$. Additionally, the peaks' areas were analyzed with principal component analysis (SIMCA-P+11; Umetrics) using autoscaled analysis, where all input variables' variances were renormalized to unit variance. This normalization provides a reliable identification of variation in metabolites with low concentration that normally would not be detectable by the naked eye [19,24]. When grouping was observed in the score plots, loading plots were analyzed to identify the integral regions with major importance in the separation of the groups.

3. Results

Histopathological analysis showed the expected dystrophic characteristics in *mdx* mice, such as variation in the fiber size, centronucleated and splitting fibers, infiltration by connective tissue and inflammatory cells, and foci of regenerated fibers. The diaphragm muscle was clearly more degenerated than the quadriceps muscle in the *mdx* strain. Muscles from the same lineage presented the same pattern in different ages and could not be distinguished by qualitative histological analysis (Fig. 1). The masses of lyophilized samples varied between 3.3 and 10.8 mg for quadriceps and between 0.7 and 1.7 mg for diaphragm. This variation justified the normalization of the spectra by the total area.

The obtained spectra were predominantly composed of narrow peaks associated with low-molecular-weight metabolites. Fig. 2 shows partial spectrum (aliphatic region) to demonstrate the signal to noise ratio. In order to not overload the spectrum, only selected peaks were singled out. However, all the 24 chemical shifts corresponding to 20 metabolites are listed in Table 1. Some overlapping peaks were observed, and their identifications were acquired based on COSY spectra (Fig. 3). Broad lines were hardly observed due to the sample preparation method which does not favor the solubilization of lipids.

The direct comparison of peak areas showed only a few differences between the groups analyzed (Table 2). The masses of diaphragm samples were extremely limited; therefore, the signal to noise ratio was not high enough for a good evaluation of some metabolites with lower concentrations, as can be seen in Table 2 (standard deviations are comparable and in some cases greater than the measured area). In order to improve the signal to noise ratio, one should use a spectrometer with a much higher magnetic field. We used a low-field magnet (4.7 T) since we are interested in implementing a similar study in vivo for DMD. The higher commercial whole-body magnets, normally available in hospitals, have magnetic fields of the order of 3 T.

In the direct comparison for quadriceps samples, only the peak 12 was different between control and *mdx* mice at 6 months of age, and the peak 15 presented reduction with aging for *mdx* mice. For diaphragm samples, the peaks 17 and 18 were elevated in the *mdx* mice at 6 months of age in comparison with the control mice at the same age. This analysis could not identify the metabolites that were different since the peaks that presented variations are related to several metabolites. On the other hand, animals were clearly grouped according to their metabolic profile through PCA in the scatter plots. Dystrophic mice at different ages could be distinguished from healthy animals for both quadriceps and diaphragm muscles (Fig. 4). It was also possible to distinguish animals of the same lineage at different ages (Fig. 5).

The results from PCA allow the identification of the major metabolites responsible for the grouping with the analysis of the loading plots. Table 3 summarizes the metabolites identified in the loading plots that had major importance for the grouping of dystrophic and control mice at different ages. All the differences observed in the direct comparison of peaks' areas were confirmed by PCA. Among the observed alterations, succinate and the amino acids glutamate and glutamine were consistently increased in dystrophic mice in both quadriceps and diaphragm muscles. The dipeptide carnosine was consistently decreased in *mdx* mice in both muscles. Creatine was reduced in *mdx* samples from quadriceps of 3-month-old mice and from diaphragm of 6-month-old mice. For the quadriceps samples, the metabolite glycine was decreased in the 6-month-old *mdx* mice in comparison to the control mice at the same age. For the diaphragm samples, the metabolite isoleucine was increased in *mdx* mice when compared to the control mice samples in both ages. The metabolites alanine, acetate and glycerol were increased in the dystrophic diaphragm samples from 6-month-old mice, while the metabolites taurine and methionine were decreased in the same samples in comparison to the control mice at the same age.

Table 4 summarizes the metabolites responsible for the differentiation of mice from the same lineage at different ages. In diaphragm samples, age effects were not identified in the direct comparison of peak areas or in the PCAs, as can be seen in Fig. 5 (right column). In the quadriceps samples, several alterations were observed with aging in both *mdx* and control mice. The concentrations of alanine, carnitine, creatine, glycine, taurine and glycerol were increased, while the concentrations of β-hydroxybutyrate, lipids, glutamate, glutamine and methionine were decreased in control animals at 3 months of age (Table 4). The concentrations of alanine, glycine and glycerol were increased, while the concentrations of glutamate, lipids, succinate, acetate and isoleucine were decreased in *mdx* mice at 3 months of age. This comparison shows that glutamate and lipids levels were decreased in the younger

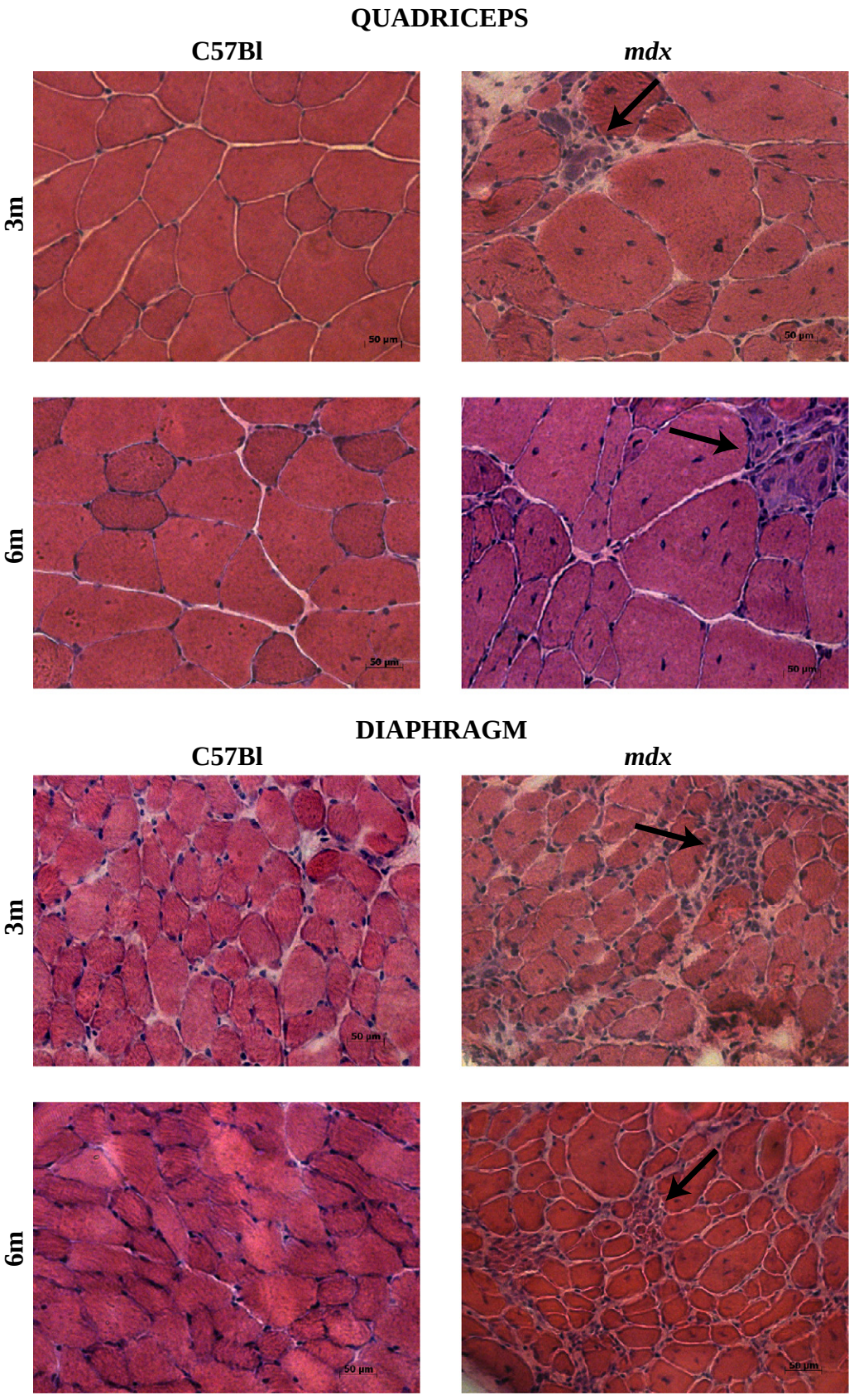

Fig. 1. Histopathological aspect of quadriceps and diaphragm muscles from control and *mdx* mice at 3 and 6 months old. Arrows indicate degeneration–regeneration foci.

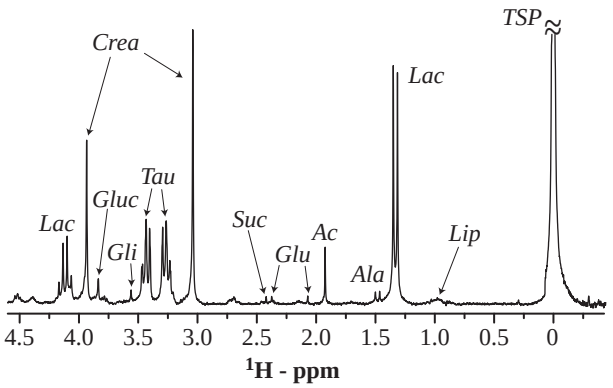

Fig. 2. A typical ^{1}H high-resolution spectrum, obtained at 200 MHz, from dystrophic muscle (quadriceps from a 6 months-old *mdx* mouse) shows the chemical shift range corresponding to aliphatic hydrogen excluding water (4.5–5.1ppm). The absorption lines due to Lactate (*Lac*), alanine (*Ala*), acetate (*Ac*), glutamate (*Glu*), succinate (*Suc*), creatine (*Crea*), taurine (*Tau*), glicine (*Gli*), glucose (*Gluc*) and lipids (*Lip*) are depicted with arrows.

mice, while alanine, glycine and glycerol were increased in younger mice for both lineages. On the other hand, the concentrations of succinate, acetate and isoleucine changed with aging for *mdx* mice but did not change for control animals. The concentrations of carnitine, creatine, taurine, β-hydroxybutyrate, glutamine and methionine did not change for *mdx* mice, but changed for control animals. The concentrations of lactate, carnosine and glucose were constant with aging in both *mdx* and control mice.

Table 1
Assignments of resonance peaks obtained from ^{1}H MRS data

Peak	Chemical shift interval (ppm)	Metabolite
1	0.78–1.09	Lipid, isoleucine
2	1.14–1.16	β-Hydroxybutyrate
3	1.17–1.20	Isoleucine
4	1.20–1.40	Lactate
5	1.44–1.52	Alanine
6	1.87–1.95	Acetate
7	2.05–2.08	Glutamate
8	2.08–2.19	Glutamine, methionine
9	2.34–2.37	Glutamate
10	2.37–2.39	Glutamate, succinate
11	2.41–2.43	Glutamine
12	2.55–2.77	Methionine, carnosine
13	3.01–3.07	Creatine, carnosine
14	3.17–3.50	Taurine, carnosine, carnitine
15	3.53–3.58	Glycine, glycerol
16	3.63–3.65	Glycerol
17	3.69–3.75	Glucose, isoleucine
18	3.78–3.87	Glutamate, glucose, glycerol, glutamine, methionine, alanine
19	3.90–3.97	Creatine
20	4.01–4.19	Lactate, β-hydroxybutyrate
21	6.12–6.21	AMP, ATP
22	7.09–7.27	Carnosine
23	8.21–8.25	AMP, ADP, ATP
24	8.51–8.59	AMP, ADP, ATP

Areas were calculated considering the indicated chemical shift intervals.

4. Discussion

The combined use of high-resolution ^{1}H NMR spectroscopy and pattern recognition methods to investigate changes associated with pathological process of cells, tissues, organs or organisms has proven to be a powerful tool for scientific investigation [17–19,22,24]. In this work, metabolomics analysis was used to identify characteristic biomarkers of dystrophic muscle tissues (quadriceps and diaphragm) and to consider the effects of aging.

The acquired spectra from all groups were relatively simple and similar, without marked differences distinguishable by the naked eye. This observation is consistent with the literature [17,21] and indicates that the absence of dystrophin and the degenerative process activated in *mdx* mice did not change significantly the major metabolites produced in muscles but may affect the regulation of the related metabolic pathways.

There were superpositions of absorption lines in spectra from different metabolites, which hampered their identification. COSY spectra were acquired to improve the identification of the metabolites related to each spectral line. Nevertheless, some peaks could not be considered in the analysis. Peak 18 (Table 1) is a superposition of absorption lines from six metabolites, some of which were presented as a single line. Therefore, the area variation from this peak could not be analyzed alone. Peaks 21, 23 and 24 could be originated from adenosine monophosphate (AMP), adenosine diphosphate (ADP) or adenosine triphosphate (ATP), so the integral variations in these peaks were not analyzed. Finally, although the peaks from lactate had great intensity in all spectra, it is not reasonable to consider it as a characteristic biomarker of the dystrophy in *mdx* mice. After the extraction and subsequent freezing of the muscles, the energetic metabolism changes from aerobic to anaerobic, thereby inducing alterations on lactate levels, which are not related to the *mdx* disorder.

The direct comparison of the peak areas was not conclusive. It was possible to identify statistical differences in some peaks, but when considering the metabolites involved, there was not a consistent pattern of changes in peaks related to the same metabolite. On the other hand, PCA showed consistent alterations, including the differences observed in the direct comparisons. Therefore, all the metabolic analyses were done with the PCA approach.

A consistent increase on glutamate and glutamine levels in *mdx* mice was observed in quadriceps and diaphragm samples. Indeed, the same behavior has already been reported by Griffin et al. [24] in dystrophic diaphragm samples. These molecules have an important role in the nitrogen metabolism, acting as nontoxic carriers of amino groups from ammonia to the liver and as sources of amino groups for the synthesis of several biomolecules, such as peptides and nucleotides [25]. It is known that high levels of glutamine can act in the protein turnover, increasing protein synthesis and reducing protein breakdown [26]. The increase in glutamine and glutamate levels could therefore be related

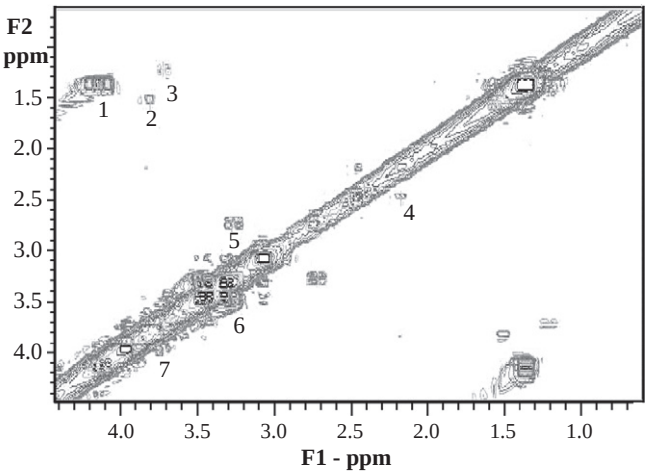

Fig. 3. Correlation spectroscopy (COSY-45) spectrum of dystrophic tissue extracted from quadriceps (6 months). 1: lactate, 2: alanine, 3: isoleucine, 4: glutamine, 5: carnosine, 6: taurine, 7: unidentified, 8: glucose.

to the requirement of protein replacement due to the intense muscle regeneration observed in *mdx* mice, mainly in limb muscles, or to a higher consumption of peptides as an energetic source to compensate for the energetic deficit observed in the dystrophic muscle.

There was also a consistent decrease in carnosine levels in *mdx* mice for quadriceps and diaphragm samples. To the best of our knowledge, this pattern has not been previously reported in *mdx* mice. Carnosine is a dipeptide consisting of β-alanine and L-histidine, with several biological functions, including antioxidant and neuroprotective activity, membrane stabilizing and regulation of metabolic processes such as protein oxidation and glycation [27]. The concentration of carnosine is particularly high in excitable tissues such as muscle and brain [28], and decreases with aging in humans and rats and also in patients with amyotrophic lateral sclerosis, myasthenia gravis, polymyositis, drug-induced myopathies and late-onset mitochondrial myopathy. This reduction is considered to be related with the muscle mass loss observed both in aging and in some neuromuscular diseases [29]. The reduction in carnosine levels in the *mdx* mice muscles observed in the present work would lead to a reduced antioxidant protection, and it could be related to the degenerative process observed in the *mdx* mice. Carnosine is also a major inhibitor of histidine decarboxylase [30] which is an enzyme that catalyzes the production of histamine from histidine amino acids. Reduction of carnosine levels would induce a higher activity of histidine decarboxylase and, consequently, a higher production of histamine. This is consistent with the continuous inflammatory process observed in the muscles of *mdx* mice.

Taurine levels were decreased in *mdx* animals when compared to the control group in the diaphragm samples from 6-month-old mice. A similar behavior has been reported by McIntosh et al. for 3-month-old *mdx* mice using ex vivo ^{1}H NMR spectroscopy [21]. Carmerino et al. [31], using high-performance liquid chromatography (HPLC), observed lower taurine levels in cardiac, skeletal muscle and brain cells, and higher taurine levels in plasma from 6-month-old *mdx* mice. The observed reduction of taurine in *mdx* mice could be related to ruptures of cellular membrane with consequent extravasation of some cellular components or to a deficiency on the capture of taurine from plasma in *mdx* mice. Taurine presents an osmoregulatory function that helps to keep the balance of Ca^{2+} levels inside the cells, thus helping the maintenance of their integrity. Taurine can also act as a potential stabilizer of polar groups in the cellular membranes. Reduction of taurine levels could interfere with the loss of membrane stability and aggravate the membrane disruption observed in dystrophic muscle fibers.

Creatine is an important biomarker for the analysis of dystrophic tissues. We observed reduction at creatine levels in *mdx* mice for diaphragm and quadriceps samples in different ages. This reduction is in agreement with studies of muscular biopsy [22] and in vivo spectroscopy of DMD patients [16]. Studies with samples from *mdx* and control mice, using NMR spectroscopy and HPLC biochemical analysis, also observed decreased creatine levels in muscle from adult *mdx* mice [24,32]. Creatine has a major role in energetic metabolism and is mainly synthesized in the liver and transported to muscle cells by blood. Just a small fraction of creatine is produced by muscular fibers. McClure et al. [33] reported that *mdx* mice can produce creatine in muscle fiber in a higher concentration than control mice due to a positive regulation of the genes GAMT and AGAT, which are involved in creatine synthesis. Indeed, dystrophic muscle fibers lose some creatine and creatine kinase enzyme due to disruption of membrane and also present difficulties in absorbing creatine from the

Table 2
Differences observed in the direct comparison of the peaks' areas from the 1D spectra (Fig. 2)

Muscle	Peak	Comparison
Quadriceps	Peak 12: methionine, carnosine	*ctrl* 6m (0.0196±0.0019) vs. *mdx* 6m (0.0103±0.0035)
	Peak 15: glycine, glycerol	*mdx* 3m (0.0131±0.0032) vs. *mdx* 6m (0.0072±0.0025)
Diaphragm	Peak 17: glucose, isoleucine	*ctrl* 6m (−0.0053±0.0083) vs. *mdx* 6m (0.0128±0.0124)
	Peak 18: glutamate, glucose, glycerol, glutamine, methionine, alanine	*ctrl* 6m (−0.0049±0.0146) vs. *mdx* 6m (0.0381±0.0229)

The differences were considered statistically significant when $P \leq .001$, after the Bonferroni's correction for the P value. All these differences were confirmed in PCA. Due to the low masses of diaphragm samples, the signal to noise ratio was low, and therefore, in some cases, the standard deviations are comparable or greater than the measured area (see the text).
6m, 6 months; 3m, 3 months.

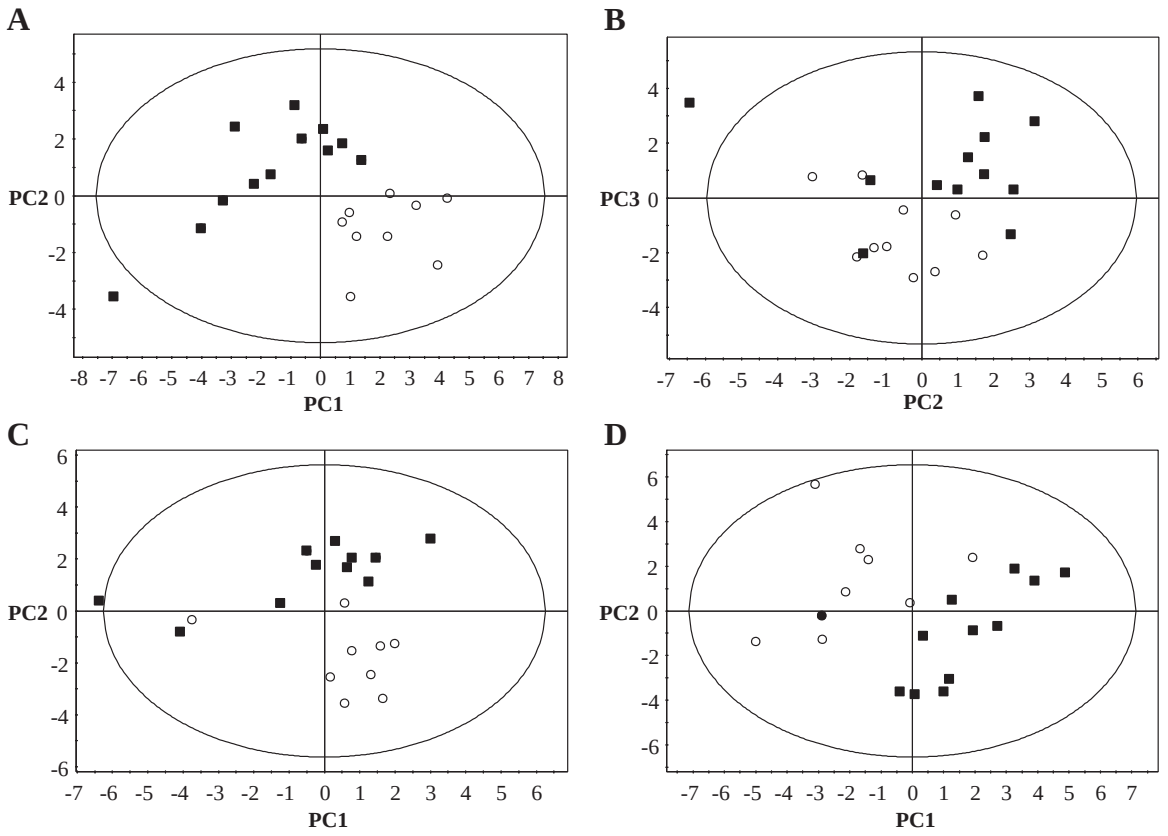

Fig. 4. Principal components analysis (*score plots*) from dystrophic and control tissues for quadriceps (*left* column) and diaphragm (*right* column) of animals at 3 months of age (A and B) and 6 of months age (C and D). Each point in the graphic represents the spectrum from one animal, and the axis indicates the scores of each spectrum in the correspondent principal component. Key: solid square, dystrophic tissue; open circle, control tissue.

bloodstream [33]. However, in *mdx* mice, this deficiency can partly be compensated with the higher production of creatine by muscle fibers. In fact, there are evidences that the concentration of creatine in *mdx* mice can be up to ~80% compared to the control [34–36], while in DMD patients, it is only 20% when compared with healthy subjects [22]. Lower levels of this metabolite have a great impact in energetic capability of muscle cells since some vital biological process, such as calcium pumps and stabilization of membrane potential, are dependent of ATP metabolism. Positive regulation on the creatine synthesis pathway in *mdx* muscle fibers could help maintain their integrity.

Succinate was elevated in *mdx* samples from diaphragm at both ages and from quadriceps at 6-month-old mice in comparison with control samples. Succinate is an intermediary in the citric acid cycle, acting in the aerobic energetic metabolism [25]. The elevation in succinate levels is observed in almost all *mdx* samples, with the exception of the quadriceps muscle from the younger *mdx* mice, the sample which presented the lower level of dystrophic features in the histology assays (Fig. 1). The elevated succinate levels and the alterations in creatine indicate that the progression of the disease is associated to changes in the energetic metabolism. Actually, it is already known that skeletal muscles from *mdx* mice and DMD patients present mitochondrial alterations and reduced activity of respiratory chain enzymes, located in the inner mitochondrial membrane, while cytosolic and mitochondrial matrix enzymes show no reduced activity [37]. The unique enzyme from the citric acid cycle in the inner membrane of the mitochondria is succinate dehydrogenase, which converts succinate to fumarate, and all the other enzymes acting in the cycle are in the mitochondrial matrix [25]. Considering this, it is possible that the dystrophic muscle accumulates succinate due to a reduced activity of all the enzymes in the mitochondrial inner membrane, particularly succinate dehydrogenase. These alterations seem to be related to the age and indicate that the evolution of the dystrophy would lead to a reduced efficacy in the aerobic metabolism. This could lead to a shift in the energetic metabolism to preferentially consume glucose in an anaerobic pathway or to prefer other energy sources, such as peptides and lipids.

Characteristics of disease evolution in *mdx* mice and natural aging in control mice are shown in Table 4. Isoleucine, succinate and acetate presented elevation with aging just in *mdx* mice. These metabolites are probably present in metabolic pathways related to the degeneration–regeneration cycles observed in *mdx* mice. For the control mice, the metabolites β-hydroxybutyrate, glutamine and methionine presented elevation with aging, while creatine, carnitine and taurine presented reduction with aging. Camerino et al. [31], using HPLC, also

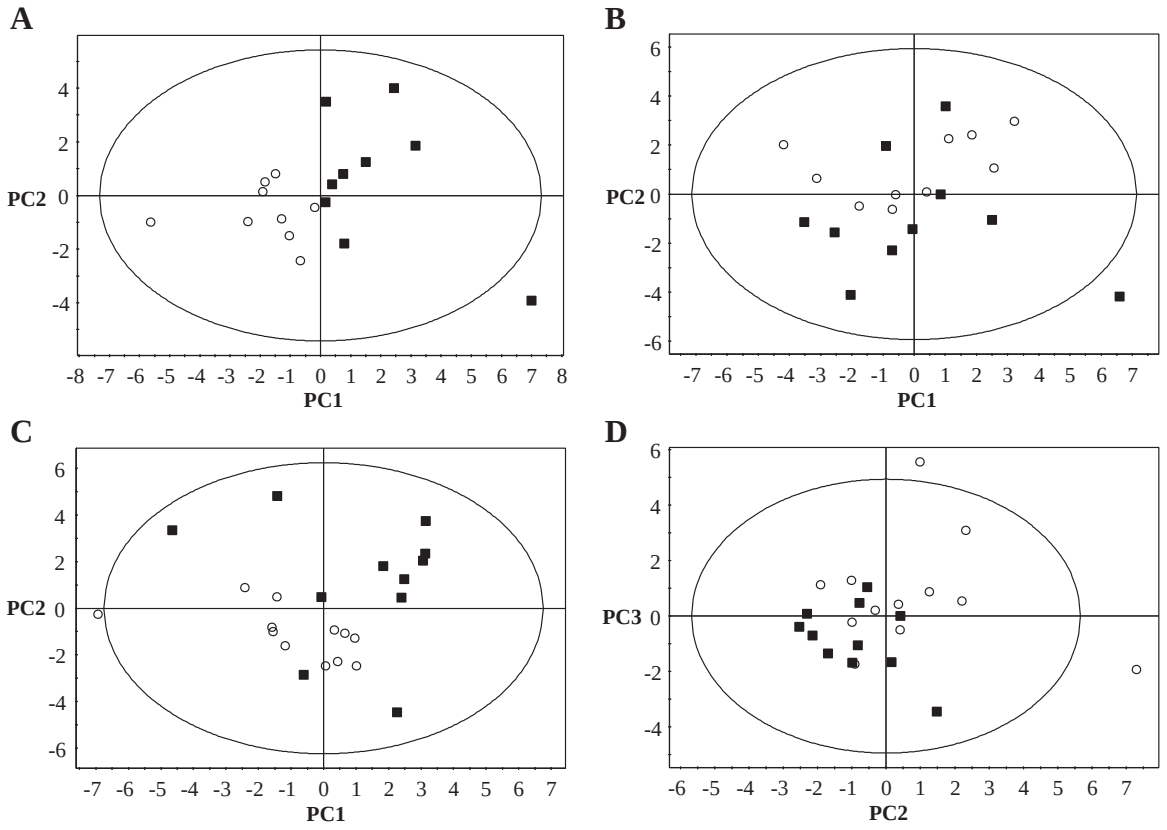

Fig. 5. Principal components analysis (*score plots*) from dystrophic and control tissues for quadriceps (*left* column) and diaphragm (*right* column) of *ctrl* (A and B) and *mdx* animals (C and D). Each point in the graphic represents the spectrum from one animal, and the axis indicates the scores of each spectrum in the correspondent principal component. Key: solid square, 6 months of age; open circle, 3 months of age.

observed a reduction of taurine concentration with aging on healthy rats. The alterations observed should not be related to necrosis or infiltration by connective tissue since the histological pattern observed in the muscles from the *mdx* and control mice is the same at both ages (Fig. 1 and Refs. [38,39]). Further studies should be done in order to characterize the involvement of these metabolites on the dystrophy progression more accurately.

No striking differences with aging were observed in diaphragm samples from control and *mdx* mice. These results signify that there is no difference in diaphragm tissue metabolism at the ages at 3 to 6 months. It is coherent with the fact that the diaphragm tissue degeneration in *mdx* mice is almost the same for 3 and 6 months of age.

McIntosh et al. [40], using ^{1}H NMR spectroscopy in extracts of the tibialis anterior and diaphragm of *mdx* and control mice, observed a decrease in the intensity of all resonance peaks of *mdx* mice compared to control ones in diaphragm samples (5 weeks old). However, the authors used the wet masses (tissue masses before lyophilization) to normalize their spectra. Considering the variation of the water content of muscle tissue due to the aging and the dystrophic process, there is a significant imprecision in this normalization procedure. Lyophilized masses would be a better parameter to normalize the spectra, but even this would lead to errors due to the highly hygroscopic nature of the product. To circumvent this problem, in this work, the spectra were normalized by the total spectra integral.

Table 3
Summary of alterations in different metabolites between *mdx* and control mice at different ages

	Quadriceps		Diaphragm	
	Higher in *mdx*	Lower in *mdx*	Higher in *mdx*	Lower in *mdx*
mdx 3mvs.*ctrl* 3m	Glutamate, glutamine	Creatine, carnosine	Glutamate, glutamine, isoleucine, succinate	Carnosine
mdx 6mvs.*ctrl* 6m	Glutamate, glutamine, succinate	Carnosine, glycine	Alanine, glutamate, acetate, glycerol, isoleucine, succinate	Creatine, carnosine, methionine, taurine

Table 4
Summary of alterations in different metabolites among animals of the same lineage at different ages in quadriceps samples

ctrl 3m vs. *ctrl* 6m		*mdx* 3m vs. *mdx* 6m	
Higher in *ctrl* 3m	Lower in *ctrl* 3m	Higher in *mdx* 3m	Lower in *mdx* 3m
Alanine, carnitine, creatine, glycine, taurine, glycerol	β-Hydroxybutyrate, lipids, glutamate, glutamine, methionine	Alanine, glycine, glycerol	Glutamate, lipids, succinate, acetate isoleucine

Sharma et al. [22] studied extracts of quadriceps samples obtained from surgical biopsy of normal and DMD patients also using ^{1}H NMR spectroscopy, and no intensity correction in the resonance spectra was performed to take into account the variability of mass. They observed a general trend in DMD patients, which was a reduction in concentration of some metabolites such as lactate, glucose, amino acids (glutamate, glutamine and alanine), glycerophosphorylcholine, phosphorylcholine, carnitine, choline, creatine and acetate. On the other hand, no metabolite showed an increase in concentration in DMD patients. Again, in this case, since DMD tissues contain much fewer muscle fibers, it is natural to expect that the spectral lines for different metabolites in these tissues would have smaller integrals than in the spectra taken from a normal tissue. Therefore, the comparison among these spectra would only be legitimate if they are normalized in some way.

Griffin et al. published several works using high-resolution ^{1}H NMR-based metabolomics approach in dystrophic mice [17,19,24]. In all these works, the resonance spectra were normalized by total area to prevent the variability of concentration in samples or changes in proportion between muscle tissue and adipose or conjunctive tissue. This is the same approach used in the present work to permit the comparison among the spectra. However, in these precedent studies, the spectra were sectioned in regular intervals of integration (typically, 0.04 ppm), producing more than 87 segments used as input variables. Such a large number of input variables require an equally large number of samples to permit a reliable analysis. Nevertheless, these studies used less than 10 animals per group. In the present paper, only the integrals under the absorption lines were taken into account, reducing the number of variables to 24, which is more compatible with the number of animals studied (10–12 samples per group). Furthermore, since just the integration interval correspondent to the signals was used, the values of peaks' areas were also normalized to present the same variance. Thus, peaks of relatively low intensity could be treated with the same importance as high-intensity peaks, without the risk of overestimation of the noise.

Finally, differences between *mdx* and *ctrl* mice with different ages could be identified by PCA on diaphragm and quadriceps samples, but few differences were detected by direct comparison between peak areas. This indicates that multivariate methods, such as PCA, are more sensitive to the metabolic alterations observed in the *mdx* mice. The observed differences should not be directly related to the dystrophin absence, but probably to secondary alterations on metabolic pathways due to alterations on the cellular membrane and to the excessive calcium influx observed in dystrophic muscular fibers, which can change the metabolic homeostasis and the osmoregulation. Furthermore, the substitution of muscle by conjunctive tissue could also change the metabolic pattern of the tissues studied.

5. Conclusions

^{1}H NMR-based metabolomics approach, associated with multivariate analysis, is a powerful tool to track possible changes in metabolite levels in the dystrophic process. The amino acids glutamate and glutamine were consistently increased in *mdx* mice, which could probably be related to the intense muscular regeneration. Succinate was also increased in *mdx* mice, which could be related to energetic alterations in the dystrophic muscle. The dipeptide carnosine was decreased in *mdx* mice, which could be related to the continuous inflammatory process. Taurine and creatine levels were reduced in *mdx* mice samples, which could be related to the degeneration process due to the dystrophy. Future studies are necessary to elucidate the metabolic pathways related to the degenerative and regenerative processes in *mdx* mice.

Acknowledgments

The authors would like to thank the following researchers for scientific and technical support: Dr. Nestor Caticha, Dr. Paulo Artaxo and Dr. Paulo Alberto Otto for the discussion about the statistical analysis; Dr. Ronaldo Nogueira de Moraes Pitombo and Gledson Manso Guimarães for the aid in the lyophilization process; and Marta Canovas and Dr. Claudia Madalena Cabrera Mori for the technical support. This work was supported by Fundação de Amparo a Pesquisa do Estado de São Paulo, Conselho Nacional de Desenvolvimento Científico e Tecnológico and Coordenação de Aperfeiçoamento de Pessoal de Nivel Superior.

References

[1] Emery AEH. The muscular dystrophies. Lancet 2002;359(9307): 687–95.
[2] Bach ABM. Estudo da distrofia muscular em camundongos mdx com ressonância magnética nuclear. Mestrado. São Paulo: Universidade de São Paulo; 2010. p. 126. http://www.teses.usp.br/teses/disponiveis/43/43134/tde-14052010-111406/pt-br.php.
[3] Chandrasekharan K, Martin PT. Genetic defects in muscular dystrophy. Methods Enzymol 2010;479:291–322 Functional glycomics.

[4] Anderson JL, Head SI, Rae C, Morley JW. Brain function in Duchenne muscular dystrophy. Brain 2002;125:4–13.
[5] Hoffman EP, Brown RH, Kunkel LM. Dystrophin — the protein product of the Duchenne muscular-dystrophy locus. Cell 1987;51(6):919–28.
[6] Gorecki DC, Monaco AP, Derry JMJ, Walker AP, Barnard EA, Barnard PJ. Expression of 4 alternative dystrophin transcripts in brain-regions regulated by different promoters. Hum Mol Genet 1992;1(7): 505–10.
[7] Yoshida M, Ozawa E. Glycoprotein complex anchoring dystrophin to sarcolemma. J Biochem 1990;108(5):748–52.
[8] Campbell KP, Stull JT. Skeletal muscle basement membrane–sarcolemma–cytoskeleton interaction minireview series. J Biol Chem 2003;278(15):12599–600.
[9] Rando TA. The dystrophin–glycoprotein complex, cellular signaling, and the regulation of cell survival in the muscular dystrophies. Muscle Nerve 2001;24(12):1575–94.
[10] Dubowitz V, Sewry CA. In: Elsevier S-, editor. Muscle biopsy — a practical approach; 2007. Printed in China.
[11] Vainzof M, Ayub-Guerrieri D, Onofre PCG, Martins PCM, Lopes VF, Zilberztajn D, et al. Animal models for genetic neuromuscular diseases. J Mol Neurosci 2008;34(3):241–8.
[12] Bulfield G, Siller WG, Wight PAL, Moore KJ. X-chromosome-linked muscular-dystrophy (Mdx) in the mouse. Proc Natl Acad Sci U S A-Biol Sci 1984;81(4):1189–92.
[13] Stedman HH, Sweeney HL, Shrager JB, Maguire HC, Panettieri RA, Petrof B, et al. The Mdx mouse diaphragm reproduces the degenerative changes of Duchenne muscular-dystrophy. Nature 1991;352(6335): 536–9.
[14] Chakkalakal JV, Thompson J, Parks RJ, Jasmin BJ. Molecular, cellular, and pharmacological therapies for Duchenne/Becker muscular dystrophies. FASEB J 2005;19(8):880–91.
[15] Hoffman EP, Dressman D. Molecular pathophysiology and targeted therapeutics for muscular dystrophy. Trends Pharmacol Sci 2001;22(9):465–70.
[16] Hsieh T-J, Jaw T-S, Chuang H-Y, Jong Y-J, Liu G-C, Li C-W. Muscle metabolism in Duchenne muscular dystrophy assessed by in vivo proton magnetic resonance spectroscopy. J Comput Assist Tomogr 2009;33(1):150–4.
[17] Griffin JL, Sang E, Evens T, Davies K, Clarke K. Metabolic profiles of dystrophin and utrophin expression in mouse models of Duchenne muscular dystrophy. FEBS Lett 2002;530(1–3):109–16.
[18] Griffin JL. Metabolic profiles to define the genome: can we hear the phenotypes? Philos Trans R Soc Lond B Biol Sci 2004;359(1446): 857–71.
[19] Griffin JL, Williams HJ, Sang E, Nicholson JK. Abnormal lipid profile of dystrophic cardiac tissue as demonstrated by one- and two-dimensional magic-angle spinning H-1 NMR spectroscopy. Magn Reson Med 2001;46(2):249–55.
[20] Jones G, Sang E, Goddard C, Mortishire-Smith RJ, Sweatman BC, Haselden JN, et al. A functional analysis of mouse models of cardiac disease through metabolic profiling. J Biol Chem 2005;280(9):7530–9.
[21] McIntosh L, Granberg KE, Briere KM, Anderson JE. Nuclear magnetic resonance spectroscopy study of muscle growth, mdx dystrophy and glucocorticoid treatments: correlation with repair. NMR Biomed 1998;11(1):1–10.
[22] Sharma U, Atri S, Sharma MC, Sarkar C, Jagannathan NR. Skeletal muscle metabolism in Duchenne muscular dystrophy (DMD): an in-vitro proton NMR spectroscopy study. Magn Reson Imaging 2003;21(2):145–53.
[23] Srivastava NK, Pradhan S, Mittal B, Gowda GAN. High resolution NMR based analysis of serum lipids in Duchenne muscular dystrophy patients and its possible diagnostic significance. NMR Biomed 2010;23(1):13–22.
[24] Griffin JL, Williams HJ, Sang E, Clarke K, Rae C, Nicholson JK. Metabolic profiling of genetic disorders: a multitissue (1)H nuclear magnetic resonance spectroscopic and pattern recognition study into dystrophic tissue. Anal Biochem 2001;293(1):16–21.
[25] Nelson DL, Lehninger MMC. Principles of biochemistry. New York: W.H. Freeman and Company; 2005. p. 656–86.
[26] Wu G. Amino acids: metabolism, functions, and nutrition. Amino Acids 2009;37(1):1–17.
[27] Boldyrev AA, Stvolinsky SL, Fedorova TN, Suslina ZA. Carnosine as a natural antioxidant and geroprotector: from molecular mechanisms to clinical trials. Rejuvenation Res 2010;13(2–3):156–8.
[28] Hipkiss AR. Would carnosine or a carnivorous diet help suppress aging and associated pathologies? Understanding and modulating aging. Ann N Y Acad Sci 2006;1067:369–74.
[29] Stuerenburg HJ. The roles of carnosine in aging of skeletal muscle and in neuromuscular diseases. Biochemistry-Moscow 2000;65(7): 862–5.
[30] Guirard BM, Snell EE. Purification and properties of pyridoxal-5′-phosphate-dependent histidine decarboxylases from *Klebsiella planticola* and *Enterobacter aerogenes*. J Bacteriol 1987;169(9):3963–8.
[31] Camerino DC, Tricarico D, Pierno S, Desaphy JF, Liantonio A, Pusch M, et al. Taurine and skeletal muscle disorders. Neurochem Res 2004;29(1):135–42.
[32] Dunn JF, Frostick S, Brown G, Radda GK. Energy status of cells lacking dystrophin — an in vivo in vitro study of Mdx mouse skeletal-muscle. Biochim Biophys Acta 1991;1096(2):115–20.
[33] McClure WC, Rabon RE, Ogawa H, Tseng BS. Upregulation of the creatine synthetic pathway in skeletal muscles of mature mdx mice. Neuromuscul Disord 2007;17(8):639–50.
[34] Louis M, Raymackers JM, Debaix H, Lebacq J, Francaux M. Effect of creatine supplementation on skeletal muscle of mdx mice. Muscle Nerve 2004;29(5):687–92.
[35] McIntosh LM, Baker BE, Anderson JE. Magnetic resonance imaging of regenerating and dystrophic mouse muscle. Biochem Cell Biol 1998;76(2–3):532–41.
[36] Dunn JF, Tracey I, Radda GK. A P-31-NMR study of muscle exercise metabolism in mdx mice — evidence for abnormal pH regulation. J Neurol Sci 1992;113(1):108–13.
[37] Kuznetsov AV, Winkler K, Wiedemann FR, von Bossanyi P, Dietzmann K, Kunz WS. Impaired mitochondrial oxidative phosphorylation in skeletal muscle of the dystrophin-deficient mdx mouse. Mol Cell Biochem 1998;183(1–2):87–96.
[38] Pastoret C, Sebille A. Mdx mice show progressive weakness and muscle deterioration with age. J Neurol Sci 1995;129(2):97–105.
[39] Roig M, Roma J, Fargas A, Munell F. Longitudinal pathologic study of the gastrocnemius muscle group in mdx mice. Acta Neuropathol 2004;107(1):27–34.
[40] McIntosh LM, Garrett KL, Megeney L, Rudnicki MA, Anderson JE. Regeneration and myogenic cell proliferation correlate with taurine levels in dystrophin- and MyoD-deficient muscles. Anat Rec 1998;252(2):311–24.